

# RSC Advances



This article can be cited before page numbers have been issued, to do this please use: S. G. and K. Sreekumar, *RSC Adv.*, 2016, DOI: 10.1039/C6RA15548K.



This is an *Accepted Manuscript*, which has been through the Royal Society of Chemistry peer review process and has been accepted for publication.

*Accepted Manuscripts* are published online shortly after acceptance, before technical editing, formatting and proof reading. Using this free service, authors can make their results available to the community, in citable form, before we publish the edited article. This *Accepted Manuscript* will be replaced by the edited, formatted and paginated article as soon as this is available.

You can find more information about *Accepted Manuscripts* in the [Information for Authors](#).

Please note that technical editing may introduce minor changes to the text and/or graphics, which may alter content. The journal's standard [Terms & Conditions](#) and the [Ethical guidelines](#) still apply. In no event shall the Royal Society of Chemistry be held responsible for any errors or omissions in this *Accepted Manuscript* or any consequences arising from the use of any information it contains.

Journal Name

ARTICLE

## Chiral dendrigraft polymer for asymmetric synthesis of isoquinuclidines

G. Smitha, K. Sreekumar\*

Received 00th January 20xx,  
Accepted 00th January 20xx

DOI: 10.1039/x0xx00000x

[www.rsc.org/](http://www.rsc.org/)

Synthesis of Multi-arm Star Dendrigraft amidoamine polymer with pentaerythritol initiated polyepichlorohydrin as core, PEN-G2 has been demonstrated on a solid resin support. We have functionalized Merrifield resin support with polyepichlorohydrin and dendrons are grown on it up to second generation using a “graft from” approach. The estimation of amine functionality was done and found to be 25 mmol<sup>-1</sup> which was 70 % of the theoretical value. Photolytic cleavage of dendrigraft polymer from the support resulted in brown water soluble viscous liquid. The molecular weight of 3966 shows that out of the 9 G1 dendritic substituents, 5 of them got converted to generation G2. TEM image of G2 polymer shows inhomogeneous polygon like appearance. The chiral modification of dendrigraft polymer, PEN-G2 has been done. The copper complex of chiral modified PEN-G2 dendrigraft polymer was synthesized and characterized. The copper complex of PEN-G2 dendrigraft polymer was found to be an excellent catalyst for the synthesis of isoquinuclidines via Aza Diels-Alder reaction between cyclohexenone and imines. The catalyst exhibited superior enantioselectivity. Reusability of the catalyst was studied for five reaction cycles.

### 1. Introduction

The term Dendronized or Dendrigraft polymer has emerged as a new concept in macromolecular design and materials science due to the unique structures which are seldom achieved by dendrimers and linear polymers.<sup>1</sup> The term dendronized polymer is assigned to polymers having linear type core while the term dendrigraft polymer is applicable to branched core polymers. Reactive oligomers or polymers are used to produce dendrigrafts or dendronized polymers, instead of using monomers, as if in constructing dendrimers. The lengthy purification procedure for the synthesis of these dendritic polymers directs us to use “solid phase strategy”. Solid phase synthesis is really a challenge, because of the large number of reactions that take place simultaneously during the building up of each generation and the number increases exponentially with increase in generation. Conversely, solid phase synthesis provides some inherent advantages over orthodox solution synthesis.<sup>2</sup> Synthesis of dendritic polymers need large excess of reagents for obtaining high purity and defect free products and solid phase synthesis usually use large excess of reagents.

Purification of intermediates is easy in solid phase synthesis, which is the most difficult and time-consuming process in solution phase synthesis of dendritic polymers. In addition, the solid resins on which the dendritic polymer is synthesized can be used as highly functionalized heterogeneous catalyst<sup>3</sup> and also as highly loaded resin for combinatorial library synthesis, with particular emphasis on one bead one compound approach.<sup>4</sup>

Recently, we reported solid phase synthesis of PAMAM dendrigraft polymer having glycerol initiated polyepichlorohydrin core, which was the first dendrigraft polymer on insoluble support.<sup>3</sup> In 1997, Bradley and co-workers introduced the solid phase synthesis of PAMAM dendrimers on organic polymer support.<sup>5</sup> Initially, the dendrons were prepared on Tentagel<sup>R</sup> up to the fourth generation. The assembly of the dendrons followed the divergent synthetic strategy developed by Tomalia *et al.* for PAMAM dendrimers in solution.<sup>6</sup> It was based on alternating steps of double Michael addition of terminal primary amines to methyl acrylate and aminolysis of the terminal esters formed with 1,2-alkanediamines. Later, the approach was extended to PAMAM dendrons on polystyrene beads equipped with a short PEG spacer.<sup>7</sup> The reaction proceeded smoothly for the synthesis of first and second generation dendrimers. Third and fourth generation dendrimers showed defect structures as observed from ESI MS data. These dendritic resins were used as high load resins for the synthesis of various molecules.<sup>8</sup> The present approach to synthesize dendrigraft polymers includes similar strategy of Michael addition and amination, but follows

Department of Applied Chemistry, Cochin University of Science and Technoogy, Kochi- 22, Kerala, India. E-mail: [kskpolymer.cusat@gmail.com](mailto:kskpolymer.cusat@gmail.com), Tel: +91-484-2575804 (Off), +91-9447121530, +91-9447053021.

Electronic Supplementary Information (ESI) available: [GPC profile, IR, NMR, Solid state <sup>13</sup>C NMR, EDX and MALDI spectrum. SEM, TEM, AFM images. Experimental procedure, Spectral data of products.

fewer steps and more number of branches compared to conventional PAMAM dendrimer. To the best of our knowledge, this is one of the few attempts to synthesize Dendrigraft polymers having branched polymeric core on a resin support other than the one reported earlier.<sup>3</sup> Most of the reports were about single core high generation dendritic systems.<sup>9</sup> So far, no report has appeared on the synthesis of amidoamine polymer on a polymeric core. Our aim was to synthesize dendritic systems having large amount of functionality even in the low generation level and we have adopted a 'graft from strategy' to synthesize these systems using polymeric core on Merrifield resin.

The amine capacity of Merrifield resin supported PAMAM dendrimers reported earlier, was found to be between 1 and 2 mmols g<sup>-1</sup> for G0 to G3 generations.<sup>9n</sup> So here, we have tried to increase the amine capacity even at the low generation level by incorporating an oligomeric core. For this purpose, we have selected pentaerythritol initiated polyepichlorohydrin (PECH) as core, coupled to the Merrifield resin and amidoamine dendrons were made to grow on it. As a result large number of amidoamine groups can be incorporated in a single step as well as in low generation. After the facile synthesis, photolytic cleavage of the resin gives a broad understanding of the structure of the synthesised polymer.

Asymmetric reactions using chiral catalysts provide the most promising method for construction of chiral molecules.<sup>10</sup> Catalytic aza Diels-Alder reaction is one of the useful methods for the synthesis of chiral nitrogen containing heterocycles.<sup>11</sup> Using aza Diels-Alder reaction, we can synthesize isoquinuclidines (azabicyclo [2.2.2] octanes) having N-bicyclic structures. They are the structural elements of numerous naturally occurring alkaloids with interesting biological properties.<sup>12</sup> A number of chiral Lewis acids and chiral Brønsted acids, as organocatalysts were reported for the activation of imine functional groups.<sup>13</sup> In particular, chiral phosphoric acid based organocatalyst was used for the activation of imine functional group which resulted in a number of asymmetric additions of various nucleophiles to imines.<sup>14</sup> In 1996, Kobayashi *et al.* reported the first examples of catalytic asymmetric aza Diels-Alder reaction using a chiral ytterbium catalyst.<sup>15</sup> Later, they reported<sup>13d,13f,16</sup> that in the presence of 1-5 mol % of Merrifield resin supported chiral BINOL zirconium catalyst, aza Diels-Alder reaction proceeded smoothly to afford the corresponding piperidine derivatives in high yields with high enantioselectivities.<sup>13e</sup> Silane Lewis acid is effective for the enantioselective promotion of aza Diels-Alder reaction of acylhydrazones with Danishefsky's diene, adding to the versatility of the family of silicon Lewis acids.<sup>17</sup> An efficient synthesis of hexahydropyrrolo[3,2-c]quinolin-2-ones and hexahydropyridino[3,2-c]quinolin-2-ones has been developed in moderate to high yields by one-pot two-step aza Diels-Alder reaction. The hexahydropyrrolo[3,2-c]quinolin-2-ones were formed as a single *exo*-stereoisomer in most cases and hexahydropyridino[3,2-c]quinolin-2-ones were formed as a mixture of *exo*- and *endo*-isomers favoring the *endo*-diastereomer.<sup>18</sup> The chiral *N,N'*-dioxide-Yb(OTf)<sub>3</sub> complex-catalyzed enantio-selective aza Diels-Alder reaction of

Brassard's diene with aldimines has been developed, giving the corresponding  $\alpha, \beta$ -unsaturated  $\delta$ -lactam derivatives in moderate yields with good enantioselectivities under mild conditions. Isolation of the reaction intermediate indicates that this asymmetric aza Diels-Alder reaction proceeds through a stepwise Mannich-type pathway.<sup>19</sup> Catalytic asymmetric Diels-Alder reaction of  $\alpha$ -amino-*o*-quinodimethane with  $\alpha, \beta$ -unsaturated aldehydes was achieved with high diastereo- and enantioselectivities in the presence of L-proline, which acts as a promoter to generate the quinodimethane from the corresponding precursor as well as a chiral catalyst.<sup>20</sup>

To date, there have been only a few reports regarding direct aza hetero-Diels-Alder reaction of cyclohexenone with aromatic aldimines. The amino acid catalyzed asymmetric aza Diels-Alder reaction between aqueous formaldehyde, unsaturated cyclic ketones, and aromatic amines furnished the desired azabicyclic ketones (24-48h) with >99% ee.<sup>21</sup> A chiral phosphoric acid, derived from 3,3-di(4-chlorophenyl)-H<sub>8</sub>-binol, exhibited superior enantioselectivity, affording fairly good yields for the reaction of a range of aromatic aldimines with cyclohexenone within 6 days.<sup>22</sup> Co(III) anionic complexes of Schiff bases obtained from salicylaldehydes and enantiomerically pure amino acids act as a novel chiral Brønsted acid to catalyze aza Diels-Alder reaction in CCl<sub>4</sub>.<sup>23</sup>

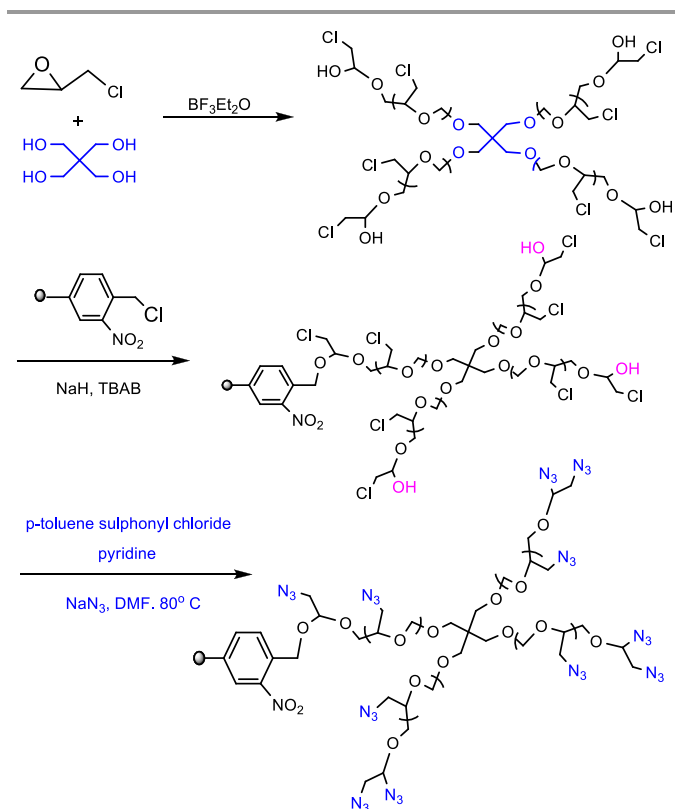
Polymer-supported Lewis acids are known to catalyze cycloadditions and polymer-loaded or dendrimer-loaded copper catalysts have been reported to be promoters of Diels-Alder reactions.<sup>24</sup> Menger *et al.* described the synthesis of polystyrene-based metallo-polymers containing copper and their use as catalysts in Diels Alder reaction.<sup>25</sup> Results suggest that metallo-polymers give better yields than the respective metal complex. Chow *et al.* reported the synthesis of dendritic bis(oxazoline)/Cu(II) complexes and their use as catalysts in the Diels-Alder reaction.<sup>26</sup> The size of the dendrimers had a strong influence on the kinetics of the reaction with a possible folding-back of the dendritic sectors towards the metallic site for higher-order dendrimers. Fujita *et al.* reported the use of dendritic bipyridines D<sub>n</sub> as ligands for Cu(OTf)<sub>2</sub> in the Diels-Alder reaction of various dienes and dienophiles.<sup>27</sup>

While, rather fruitful results have been reported in catalytic asymmetric Diels-Alder reactions,<sup>10-11,23,28</sup> successful results are limited in asymmetric aza Diels-Alder reactions using dendritic systems. Amino acid derivatives were well-known for enantioselective Diels-Alder reaction.<sup>13m,29</sup> These results<sup>30</sup> have led us to investigate whether an amino acid-metal complex of dendritic system could be able to mediate the classical aza Diels-Alder reaction through a catalytic enamine mechanism. Herein, we report the direct catalytic aza Diels-Alder reaction of cyclohexenone with aldimines, achieved with good diastereo and enantioselectivities in the presence of a copper complex of proline modified dendrigraft polymer supported on Merrifield resin.

## 2. Results and discussion

### 2.1 Characterization of PEN-G2 polymer

The resin supported dendrigraft azide polymer was synthesized using the schematic procedure (Scheme 1).



**Scheme 1** Synthesis of resin supported azide polymer

The branched hydroxyl terminated PECH (polyepichlorohydrin) was prepared by the ring opening polymerization of the oxirane group in ECH (epichlorohydrin) in the presence of pentaerythritol by activated monomer mechanism (AMM).<sup>31</sup> It was a light yellow viscous liquid. From GPC, the molecular weight of PECH was found to be 1037 with polydispersity index of 1.27. The <sup>1</sup>H NMR spectrum indicated that the hydroxyl groups at the terminal ends were secondary in nature.

Merrifield resin (1% cross-linked with DVB) was gifted from Thermax India Ltd. Its chlorine capacity was found to be 5.2 mmols g<sup>-1</sup>. It was made photoactive by the introduction of a nitro group at the ortho position of chloromethyl group.<sup>32</sup> The PECH was coupled to the resin using sodium hydride and tetrabutyl ammonium bromide.<sup>33</sup> After coupling, chlorine capacity was found to be 7.2 mmols g<sup>-1</sup> by Volhards method. From the scanning electron micrographs of nitrated Merrifield Resin and PECH attached Merrifield Resin, it was found that, after modification with PECH, beads with low extent of grafting were spherical with an appearance similar to the precursor resin particles. SEM EDAX showed that 18 atom% of chlorine was present in the sample.

The IR spectral data of nitrated Merrifield resin at 1596 cm<sup>-1</sup> and 1360 cm<sup>-1</sup> correspond to the stretching vibrations due to NO<sub>2</sub> group. The IR spectrum of PECH coupled Merrifield resin

showed a band at 1107 cm<sup>-1</sup> and a broad band at 3430 cm<sup>-1</sup> which corresponded to C-O-C stretching of ether linkage and due to the hydroxyl group of polyepichlorohydrin. In solid state CP MAS <sup>13</sup>C NMR spectrum, broad signal around 50-85 ppm includes CH<sub>2</sub>-OH, CH-O-CH<sub>2</sub> carbons of polyepichlorohydrin, the signal around 125 to 150 ppm is due to carbons of polystyrene support and 0-50 ppm includes carbons due to alkyl part of both support and PECH (Figure 1).

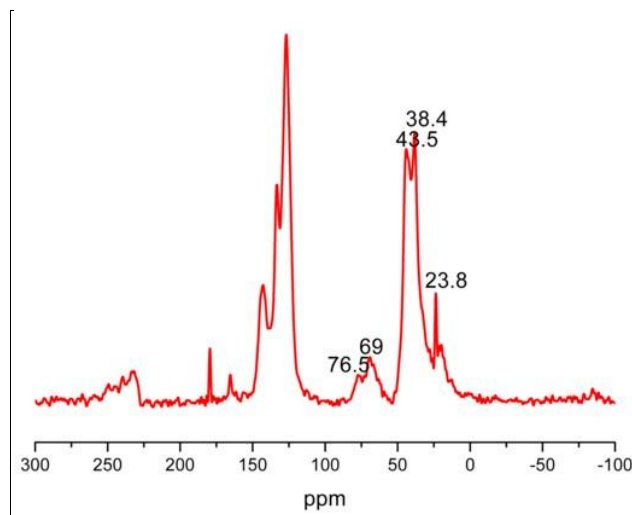


**Figure 1** Solid State CP MAS <sup>13</sup>C NMR Spectrum of PECH attached Merrifield Resin

In the TG curve of PECH attached resin, two mass loss steps were observed. The first decomposition corresponded to nearly 54 % mass loss in the temperature around 323 °C. The second stage was completed around 413 °C. The first step of mass loss in TG could be attributed to elimination of chlorinated compounds. The mass loss above 400 °C was due to the breakdown of the polymer backbone (Figure 2).<sup>34</sup>

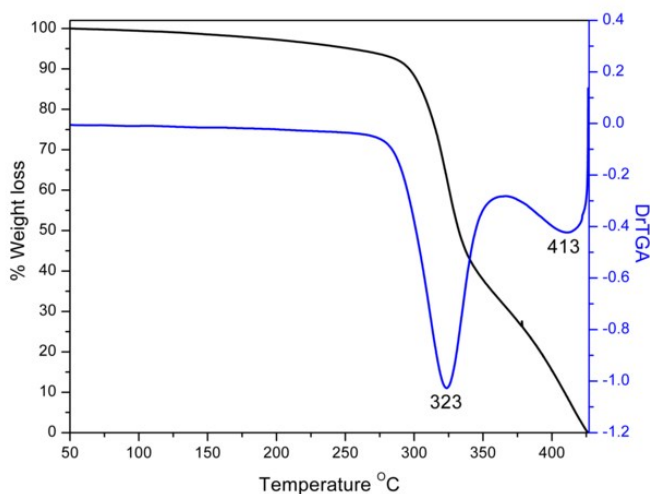
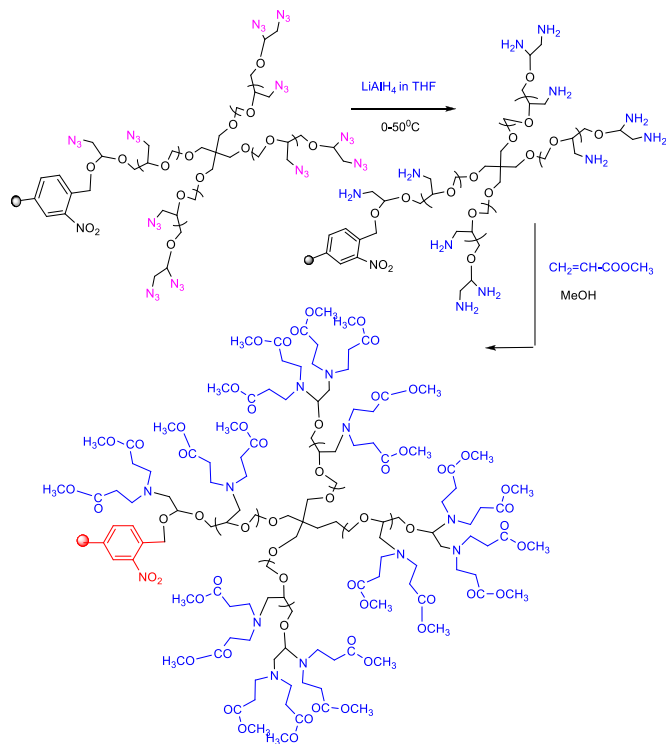


**Figure 2** TG-DTG plot of PECH loaded Merrifield Resin

These observations give clear evidence for the attachment of PECH to the Merrifield resin. The hydroxyl groups of PECH loaded resin was estimated quantitatively. The amount of hydroxyl groups was found to be  $1.86 \text{ mmol g}^{-1}$  of the polymer. The hydroxyl group of the polymer was reacted with *p*-toluene sulphonyl chloride (TsCl) in pyridine.<sup>35</sup> After tosylation, percentage of sulphur was found to be 2.44 % from CHNS data (C-68.39%, H-5.66%, S-2.44% and N-1.55%). The disappearance of broad deep peak around  $3500 \text{ cm}^{-1}$  in the IR spectrum of tosylated PECH indicated the alteration of hydroxyl group to tosyl group. During tosylation, it was observed that the yield was decreased to half by keeping the reaction for more time. This was due to the cleavage of the ether linkages in the polymer by the reaction with TsCl.<sup>36</sup> The situation was same when 4% cross-linked Merrifield resin was used. The reaction was also monitored with *p*-toluene sulphonyl chloride in triethylamine. But there was no great noticeable change with respect to the yield of the product. The azidation of tosylated PECH was carried out using sodium azide in dimethylformamide at  $85\text{--}90^\circ\text{C}$ .<sup>37</sup> An intense peak at  $2100 \text{ cm}^{-1}$  in IR spectrum indicated the presence of azide functionality. In the solid state CP MAS  $^{13}\text{C}$  NMR spectrum, due to the conversion of  $\text{CH}_2\text{-Cl}$  of PECH to  $\text{CH}_2\text{-N}_3$ , the signal at 43.5 ppm was shifted to 38.5 ppm. The colour of the resin was changed to brown. The polyazide on reduction with lithium aluminium hydride in THF got converted to  $\text{-CH}_2\text{NH}_2$  (Scheme 2).<sup>38</sup>



Scheme 2 Synthesis of G 0.5 dendrigraft polymer

In the IR spectrum of G0 polymer, the peak at  $2100 \text{ cm}^{-1}$  had completely disappeared and a peak at  $3451 \text{ cm}^{-1}$  showed

the presence of amine functionality (Figure 3). The quantitative estimation showed the presence of  $9.125 \text{ mmol}$  of amine per gram of the resin. This high amine capacity compared with previously reported polyamines could happen only if the resin was loaded with PECH.

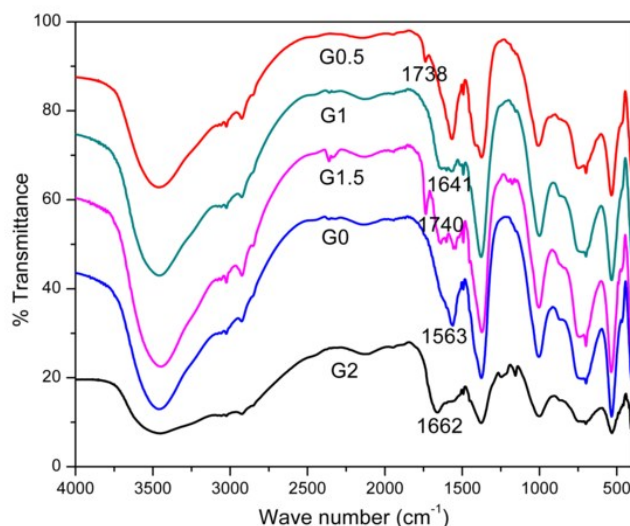


Figure 3 IR spectra of PEN-G0, PEN-G0.5, PEN-G1, PEN-G1.5, PEN-G2

Quantification of the number of amino groups from DTG result was very close to the value obtained by analytical methods (Figure 4).<sup>39</sup> In the TG trace of G0 polymer, the first mass loss of about 20 % at  $186^\circ\text{C}$  was due to the elimination of amine as molecular nitrogen. The second mass loss of about 40 % at  $404^\circ\text{C}$  was due to the degradation of polyether chains. The Michael addition of the G0 polyamine with methyl acrylate in methanol showed a peak at  $1738 \text{ cm}^{-1}$  in the IR spectrum of G0.5 (Figure 3).<sup>6</sup> Even though IR spectrum showed vibration bands in the region around  $3400 \text{ cm}^{-1}$ , negative Kaiser ninhydrin test result confirmed the absence of free amino groups.

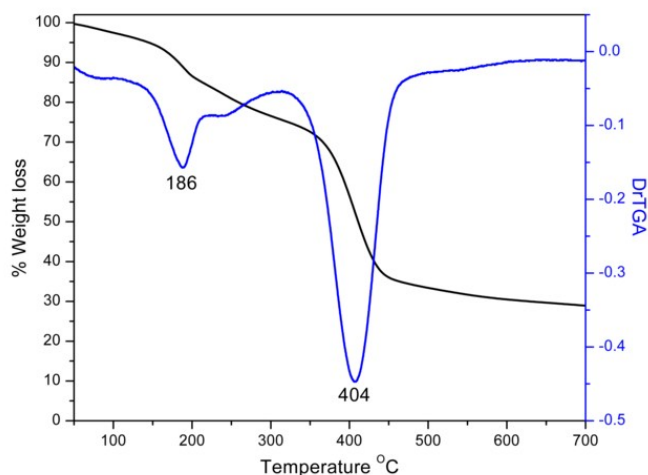
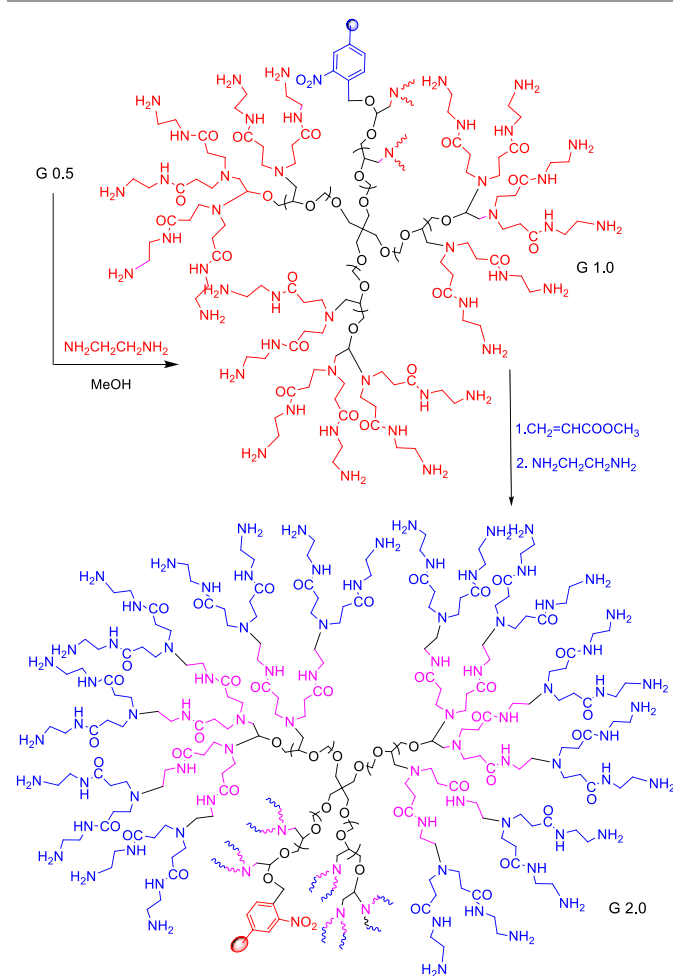


Figure 4 TG-DTG plot of PEN-G0

In the solid state CP MAS  $^{13}\text{C}$  NMR spectrum of G0.5, appearance of a peak at 169 ppm confirmed the incorporation of ester functionality. The G 0.5 polymer on amination with ethylene diamine got converted to amidoamine G1 polymer (Scheme 3).<sup>40</sup>



**Scheme 3** Synthesis of G1 and G2.0 dendrigraft polymer

In the IR spectrum of G1 polymer, bands at 1641 and 3466  $\text{cm}^{-1}$  are due to the amide carbonyl and amine moiety of the polymer (Figure 3). Both Michael addition and amination reaction took prolonged time for completion because of the poor swelling of resin loaded polymer in methanol. The amine capacity of G1 polymer was found to be 18.75  $\text{mmols g}^{-1}$ . In the TG curve of G1 resin; two mass loss steps were observed. The first decomposition corresponded to nearly 26 % mass loss in the temperature around 200  $^{\circ}\text{C}$ . The second stage mass loss of 30 % was observed around 383  $^{\circ}\text{C}$  (Figure 5). The first step of mass loss in TG can be attributed to elimination of molecular nitrogen from the amino groups. The mass loss near 400  $^{\circ}\text{C}$  was due to the thermal degradation of the polymer backbone leading to the formation of hydrogen, carbon monoxide, carbon dioxide, methane, ammonia, hydrogen cyanide gas and other higher hydrocarbons.<sup>34</sup>

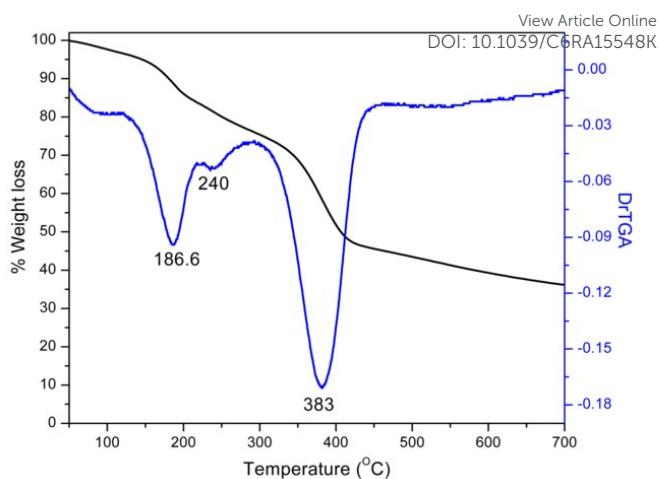


**Figure 5** TG-DTG plot of PEN-G1

The synthesis procedure was repeated to get G2 DP (Dendrigraft polymer). Michael addition of G1 polymer resulted in the conversion of G1 to G1.5 Dendrigraft Polymer. The peak at  $1641\text{cm}^{-1}$  in the IR spectrum due to carbonyl stretching of amide  $-\text{C}=\text{O}$  of PEN-G1 got converted to  $1740\text{cm}^{-1}$  after Michael addition with methyl acrylate (Figure 3). In the solid state CP MAS  $^{13}\text{C}$  NMR spectrum of PEN-G1.5, the signal at 169.4 ppm corresponds to ester carbon (Figure 6).

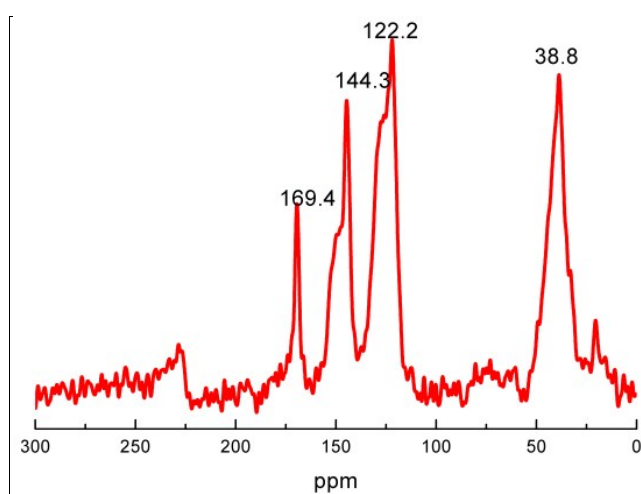


**Figure 6** Solid state CP MAS  $^{13}\text{C}$  NMR spectrum of PEN G1.5 polymer

The above G1.5 polymer on amination with ethylene diamine was converted to G2 polymer. The IR spectrum of PEN-G2 polymer showed vibration band at  $1662\text{cm}^{-1}$  due to carbonyl stretching of amide carbonyl and the band at  $1740\text{cm}^{-1}$  in the G1.5 due to ester functionality was disappeared (Figure 3). TG plot of PEN-G2 polymer showed similar decomposition pathway as that of G1 polymer, but a total mass loss of 36 % at 194.7 and 272.4  $^{\circ}\text{C}$ , and a 25 % mass loss at 407  $^{\circ}\text{C}$  had occurred (Figure 7).

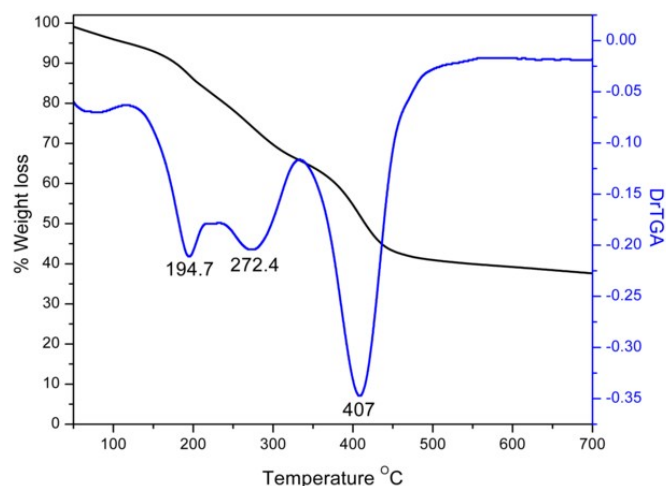


Figure 7 TG-DTG plot of PEN-G2

Scanning electron micrograph of G2 DP shows irregular agglomerates of different shapes (Figure 8). The loss of spherical nature was due to the crushing of the supported Dendrigrraft polymer due to prolonged stirring or may be due to the umbrella effect (to stretch to maximum extent) of the resin supported dendritic polymer.

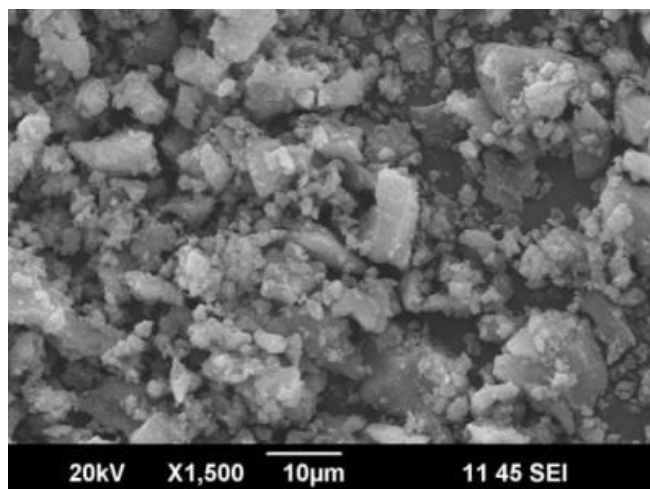


Figure 8 SEM image of PEN-G2

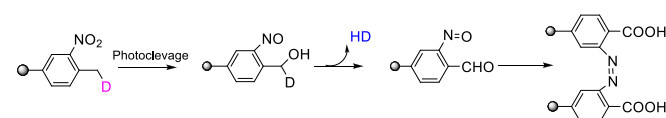
The amine capacity of G2 polymer was found to be 25 mmols  $g^{-1}$  which was not in good agreement with the theoretical value. This discrepancy is probably due to defective growth of the dendrons as a result of steric crowding and also due to hydrogen bonding which results in the lack of availability of free amine functionality for carrying out the Michael addition and subsequent reactions and also to a small extent of interpenetration of branches to one another. The amount of amino group in the G0, G1 and G2 series was found to be higher for GLR-Gn polymer than PEN-Gn polymer.<sup>3</sup> This may be due to the monodispersity and high molecular weight of glycerol initiated polyepichlorohydrin compared to

pentaerythritol initiated polyepichlorohydrin, the one reported here.

DOI: 10.1039/C6RA15548K

## 2.2 Characterization of Photolytically Cleaved PEN-G2 Dendrigrraft Polymer

Under photolytic conditions, the G0, G1 and G2 dendrigrraft polymer undergo cleavage from the support. On photolytic cleavage, the nitro group on polystyrene resin was converted to nitroso group with the elimination of dendritic polymer (Scheme 4).<sup>41</sup>



Scheme 4 Mechanism of Photolytic Cleavage

The resultant G0 polymer was a brown viscous liquid, soluble in DMSO and methanol. The Chem Bio 3D image of G0 polymer cleaved from the support is shown in the Figure 9.

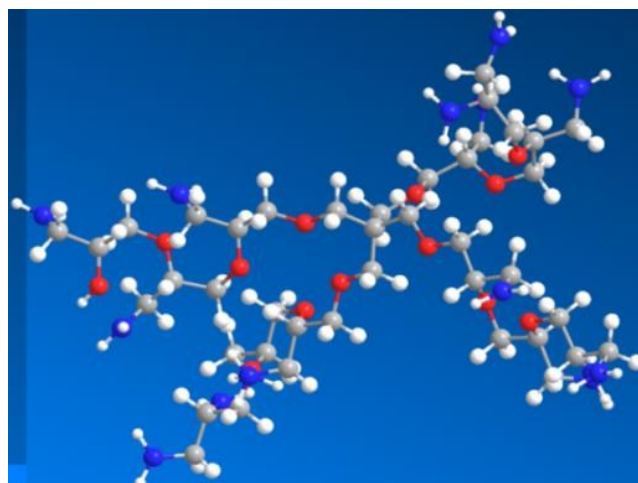


Figure 9 Chem Bio 3D image of G0 Dendrigrraft Polymer

The  $^1H$  NMR spectrum shows that the polymeric arms are somewhat similar. The appearance of peaks in the range 3.2–3.9 ppm in the  $^1H$  NMR spectrum is due to the  $CH_2-O$ ,  $CH-O$  and  $NH_2$  protons of the polymer. The observed behaviour suggests that growth is regulated by a feedback mechanism due to confinement imposed by the support.<sup>42</sup> From MALDI TOF MS analysis, the molecular weight of the polymer was found to be 884, which was agreeable with the theoretical value (Figure 10).

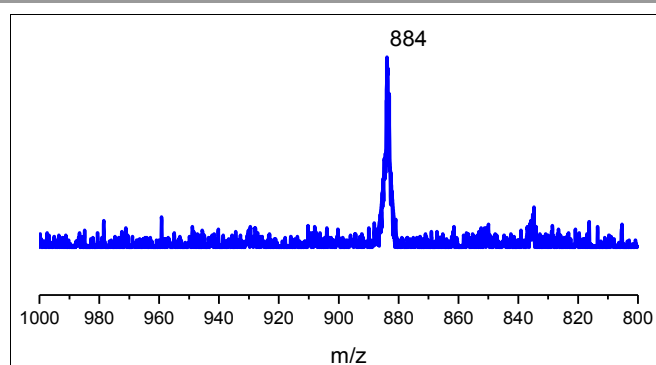


Figure 10 MALDI MS Spectrum of PEN-G0 Polymer

Resin loaded G1 polymer on photolytic cleavage gives a brown viscous liquid. One issue that needs to be addressed is the solubility of Dendronized polymers (DP). It has been known that, in general, DPs containing large number of free peripheral amine groups have low solubility in most commonly used solvents.<sup>43</sup> The lower solubility of the branched chains was attributed to their high propensity to crystallization.<sup>11</sup> Inspection of the <sup>1</sup>H NMR spectrum of the G1 DP cleaved from the resin clearly indicates the appearance of amide proton at 8.1 ppm which was absent in G0 DP. To determine the exact number of dendritic substituents introduced, MALDI-TOF MS analysis was performed (matrix: dihydroxybenzoic acid) with the dendronized PEN-G1 polymer. But polymers with polydispersity index greater than 1.2 are difficult to be characterized with MALDI MS due to the signal intensity discrimination against higher mass oligomers.<sup>44</sup> The MALDI-TOF MS of PEN-G1 exhibited several peaks. Focus may be given to two major peaks. The peak at 2857.55 Da is derived from nine dendritic substituents on a pentaerythritol initiated polyether chain. The base peak at 1664.39 Da is derived from four dendritic substituents on a pentaerythritol initiated polyether chain. These results indicate that the G0 polymer was modified to ~70 % with dendron substituents on the polyether backbone. Generally, in order to minimize defects or cyclisation and to ensure complete reaction, as we go from lower to higher generation, large molar excess of the reagents have to be taken.<sup>45</sup>

To confirm the introduction of dendritic substituents onto polyether, dendronized G1 polymer was analyzed by atomic force microscopy (AFM).<sup>46</sup> Samples for AFM analysis were prepared by spin coating methanolic solution of the dendronized polymer on a glass plate and AFM analysis was performed in the tapping mode. The AFM image of the film of G1 polymer deposited from higher concentration (0.1 % w/w) at a scan width of 75  $\mu$ m shows spherical aggregates of different sizes.

The <sup>1</sup>H NMR spectrum of PEN-G2 Dendronized polymer shows broadening of peaks in comparison with PEN-G1 DP. The occurrence of structural defects and dendritic aggregation due to the interdigitation of dendritic arms are commonly encountered during the synthesis of high generation dendritic polymers.<sup>47</sup> In this regard, defects in the dendritic structure

can arise through incomplete reactions brought about by steric congestion at the periphery or backfolding of flexible dendritic branches, which hides their functional groups. The highest molecular weight of the PEN-G2 polymer from MALDI MS analysis was found to be 3966.02 with a base peak at 1225.41 and another major peak at 1662.72. The molecular weight at 3966.02 shows that out of the 9 G1 dendritic substituents, 5 of them got converted to G2.

The peak at 1662.72 corresponds to the formation of one G2 dendron unit. The peak at 1225.41 is due to cleavage of G2 dendritic unit from the polymeric backbone. The highest mass of 3966 shows that only 30% of dendron substituents are incorporated. The low experimental mass compared to theoretical mass can be due to missing branches. The difference in experimental and theoretical masses can partially be attributed to structural defects, because, errors can also be due to the polydisperse nature of the polymer. Also, the lower mass may be due to the thermal decomposition of the high generation polymer in comparison with lower generation dendrigraft polymers.<sup>48</sup> For a comparison we tried to find out the mass of the glycerol based dendrigraft GLR-G2 polymer.<sup>49</sup> Merrifield resin carrying the GLR-G2 polymer was cleaved photolytically. The molecular weight obtained from MALDI analysis was 2927, which corresponded to 9 dendritic units on the polyether backbone.

Molecular simulation of the PAMAM dendrimers have indicated that the early full generations (G = 1-2) are characterized by asymmetric disk like shapes. These correspond to open structures that can be readily penetrated by solvent. Higher generations possess a nearly spherical shape, which corresponds to closed, densely packed surface structures.<sup>50</sup> In contrast to dendrimers, dendrigraft polymers show more closed or spherical nature at low generation, but at higher generations, polymeric arms are more stretched and have rod like appearance.<sup>51</sup>

The shape of the polymer in the case of PEN-G2 was analyzed by atomic force microscopy (AFM) as in the case of PEN-G1. In AFM, the film uniformity is mostly determined by the concentration of the dendritic solution regardless of generation.<sup>52</sup> The AFM image of the G2 polymer from lower concentration (0.01 wt%) at a scan width of 15  $\mu$ m around 10 nm shows a small elongated worm or string like appearance. Since polyether backbone is only having approximately 10-13 units, the length of the worm that we observed is agreeable with the length of the polyether oligomer. Despite the approximate nature owing to uncertainties associated with the AFM technique (tip convolution), it was clear that the average worm length corresponds to the length of the parent polyether, whereas the height of the polymer chain depends upon the dendron generation.<sup>53</sup>

The TEM micrograph of the PEN-G2 polymer shows polygon shape with low molecular weight polymers aggregate inside the polygon (Figure 11). The polygon shape with longest-extension diameter of up to 13.7 nm may be due to the clustering of polymeric arms in solution. Reports regarding dendrigraft polymers say that they are elongated due to linear

polymeric core with dendritic arms. But in solution they remain as spherical.<sup>54</sup>

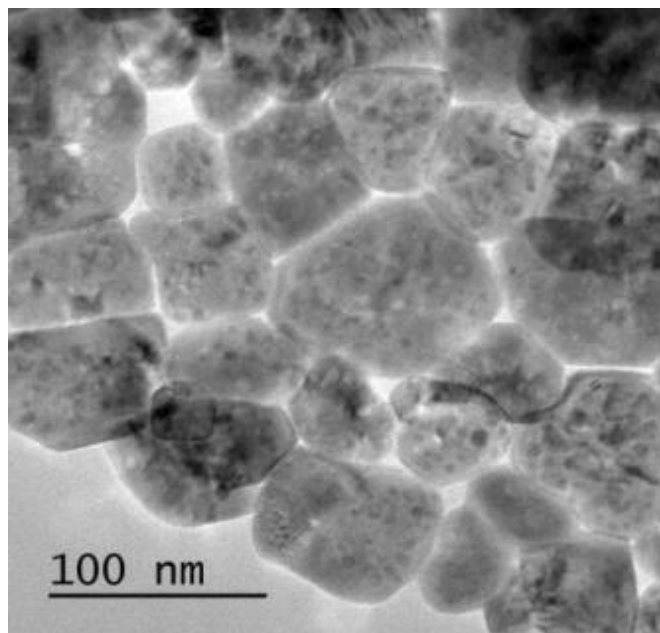
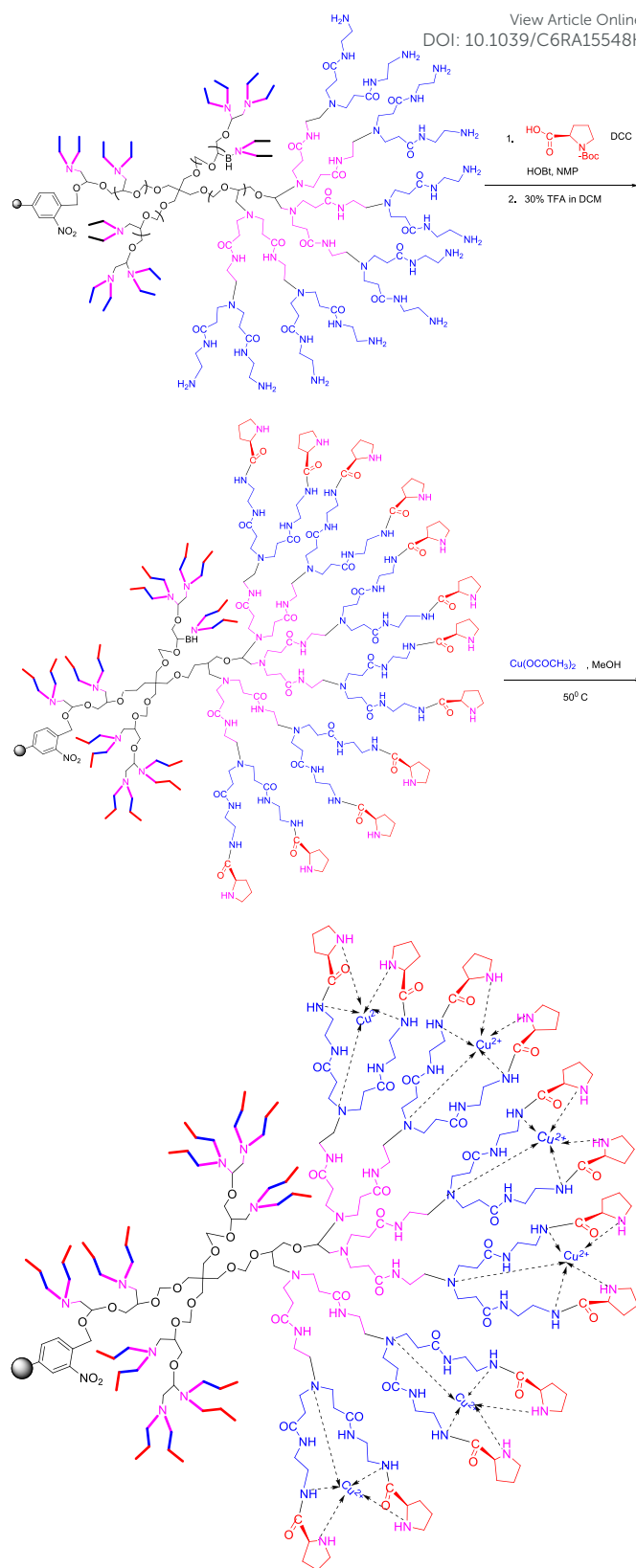


Figure 11 TEM image of PEN-G2 polymer

### 2.3 Characterization of Chiral modified dendrigraft PEN-G2 metal complex

The synthesis of the resin supported chiral modified dendrigraft PEN-Gn copper complex was achieved by adopting a three-step methodology, as shown in Scheme 5. Chiral modification of PEN-G2 polymer was done using Boc-L-proline followed by deprotection using trifluoroacetic acid. After chiral modification, amount of proline was found to be 12.54 and 20.63 mmol g<sup>-1</sup> for G1 and G2 respectively. Chiral modified dendrigraft PEN-G2 polymer was complexed with copper using copper acetate in methanol at a temperature of about 50 °C. Chiral PEN-Gn-Cu was found to be non-hygroscopic, stable and can be stored for a prolonged period of time without any change in its catalytic efficiency. The copper coordinated dendritic polymer appeared as light green powder.



Scheme 5 Chiral modification and Metal complexation of PEN-G2 polymer

#### 2.3.1 ICP-AES Analysis

The copper capacity of PEN-G1-Cu and PEN-G2-Cu, based on ICP-AES analysis and confirmed by EDX analysis, were found to be 20.40, 32.36 % of the polymer, respectively (Table 1). It is therefore assumed that an average of 2.03 ligands was bound to  $\text{Cu}^{2+}$  ions in chiral PEN-G2 complex. Acetate ions were completely replaced by the dendritic ligands. The room temperature magnetic moment of the copper (II) PEN-G2 complex was found to be 2.1B.M. The Cu compounds were paramagnetic in nature, as was evident from the magnetic susceptibility measurement, which was consistent with the presence of Cu centers in their +2 oxidation state.

**Table 1** Analytical data for chiral PEN-Gn and chiral PEN-Gn-Cu

Polymer	Proline NH capacity (mmol/g)	Copper (%) ICP-AES	Copper (mmol/g) ICP-AES	Copper (%) EDX
Chiral PEN-G1-(Cu)	12.54	20.40	3.21	19.23
Chiral PEN-G2-(Cu)	20.63	32.36	5.09	30.27

### 2.3.2 SEM and Energy Dispersive X-ray (EDX) Analysis

The SEM micrographs of chiral PEN-G2-Cu polymer shows disordered aggregates and aggregated particles look flattened and show metallic lustre (Figure.12). EDX spectrum confirmed the presence of Cu, C, N and O as the constituents of the polymer. The results presented in Table 6.1 are the average of the data from scanned regions. The data obtained on the composition of the compounds from the energy dispersive X-ray spectroscopy, were consistent with the elemental analysis values (Table .1).

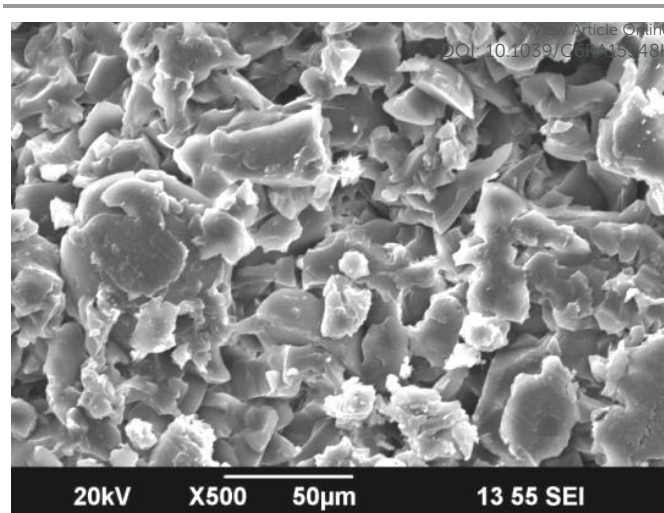


Figure 12 Scanning electron micrograph of Chiral PEN-G2-Cu

### 2.3.3 IR Spectral Studies

The IR spectra showed characteristic differences between the spectral pattern originating from the dendrigraft PEN-G2 polymer, proline modified dendrigraft PEN-G2 polymer and the corresponding copper complex. The IR spectra are presented in Figure 13. Dendrigraft PEN G2 polymer on Boc-proline modification showed bands at  $1740\text{ cm}^{-1}$  due to ester carbonyl stretching of Boc carbonyl group. On deprotection, the peak at  $1740\text{ cm}^{-1}$  got disappeared and showed only the peak due to amide at  $1692\text{ cm}^{-1}$ .

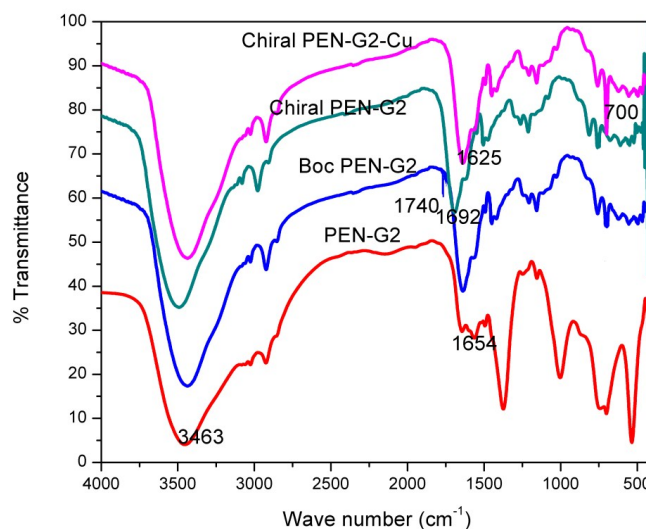


Figure 13 IR Spectra comparison for chiral modification

Proline modified polymer on complexation with copper showed a distinct shift towards lower frequency region. Stretching due to proline NH was lowered around  $64\text{ cm}^{-1}$  and that of amide carbonyl stretching was lowered from  $1692\text{ cm}^{-1}$  to  $1625\text{ cm}^{-1}$ . The peak at  $1508\text{ cm}^{-1}$  is due to stretching vibrations of secondary amine. Bending vibrations due to primary amine at  $1610\text{ cm}^{-1}$  in the PEN-G2 polymer got

modified by the secondary NH vibrations in chiral PEN-G2 polymer. The peak at  $1200\text{ cm}^{-1}$  is due to the  $\text{CH}_2$  wagging of cyclopentane ring. After chiral modification, the peak at  $1007\text{ cm}^{-1}$  in PEN-G2 due to the ethereal C-O stretching got merged with nearby peaks and shifted towards higher frequency region. The narrow peak at  $700\text{ cm}^{-1}$  can be assigned to Cu-N stretching.

### 2.3.4 Electronic Spectral Studies (UV-Vis DRS)

UV-Vis DRS spectrum of Cu complex of proline modified PEN-G2 shows two peaks with maximum intensity at 671 nm and 839 nm. The peak at 839 nm relates to a distorted octahedral geometry and the peak at 671 nm to a square pyramidal geometry characteristic of five coordinated species.<sup>55</sup> But on compilation of other characteristic data, the square pyramidal geometry may be assigned to chiral PEN-G2-Cu complex. The peak at 671 nm and 839 nm may be ascribed to the absorption due to overlapping of allowed d-d transitions in copper after coordination with dendritic ligands.

### 2.3.5 EPR Spectral Studies

EPR Spectral studies of Cu complex of proline modified PEN-G2 show typical axial spectra with four hyperfine lines, which is characteristic of monomeric copper (II) complexes. The g and A values are obtained from the simulated spectrum given in Table 2. In all the cases  $g_{\parallel}$  was found to be greater than  $g_{\perp}$ . This predicts a square pyramidal geometry to five coordinated complex rather than a trigonal bipyramidal structure which would be expected to have  $g_{\perp}$  greater than  $g_{\parallel}$ .<sup>56</sup> Thus the chiral PEN-G2-Cu comprises of coordination of copper to two proline nitrogens, two amide nitrogens and one tertiary nitrogen of amidoamine unit.

Table 2 Splitting parameters g and A

Polymer	$g_{\parallel}$	$g_{\perp}$	$g_{av}$	$A_{\parallel}$	$A_{\perp}$	$A_{av}$
PEN-G2-Cu	2.28	2.07	2.14	195	12.8	69.8 3

### 2.3.6 X-ray Diffraction Studies

The room-temperature X-ray diffraction patterns of the pentaerythritol initiated dendrigraft polymer, PEN-G2 and the Copper complex of the chiral dendrigraft polymer PEN-G2-Cu on Merrifield resins are overlaid. After chiral modification and complexation, the peaks corresponding to various 2 theta values in PEN-G2 have disappeared indicating the loss of crystalline nature of the polymer complex. This observation confirms that the copper has been anchored to the polymer matrix to yield the polymer supported dendritic copper catalyst PEN-G2-Cu.

### 2.3.7 X-ray Photoelectron Spectroscopy

Figure 14 presents the Cu (2p) XPS spectra of the PEN-G2 Cu catalyst. The catalyst displayed characteristic Cu(2p<sub>3/2</sub>) singlet with peak located at 934.6 eV. Strong satellite peaks were observed at 942.7, 954.7 and 962.6 eV. The noted binding energy values are in good agreement with the available literature data for Cu ions in the 2+ oxidation state.<sup>57</sup> The presence of Cu (II) in supported dendritic polymer has thus been confirmed from the results of XPS analysis.

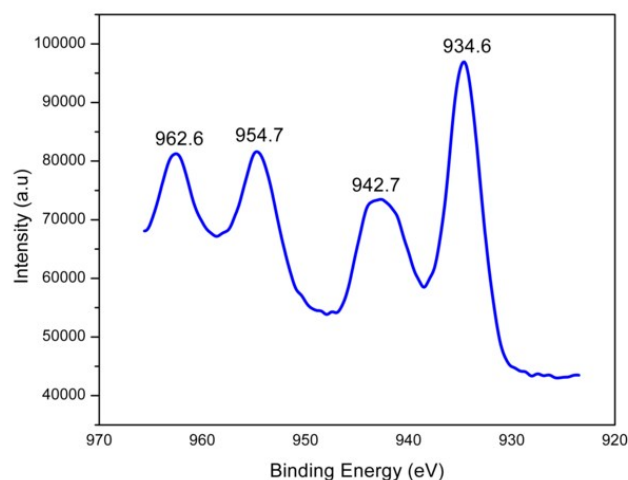


Figure 14 deconvoluted XPS spectra of Cu (2p<sub>3/2</sub>) of PEN-G2-Cu

### 2.3.8 TG-DTG Analysis

A comparative evaluation of the thermogravimetric data of the PEN-G2 functionalized resins and the corresponding Cu loaded PEN-G2 dendrigraft polymer is shown in the figure (Figure 7 & 15). An intense decomposition is observed in the thermogram of both PEN-G2 and PEN-G2-Cu at temperatures above  $400\text{ }^{\circ}\text{C}$  owing to the degradation of the polymeric backbone.<sup>58</sup>

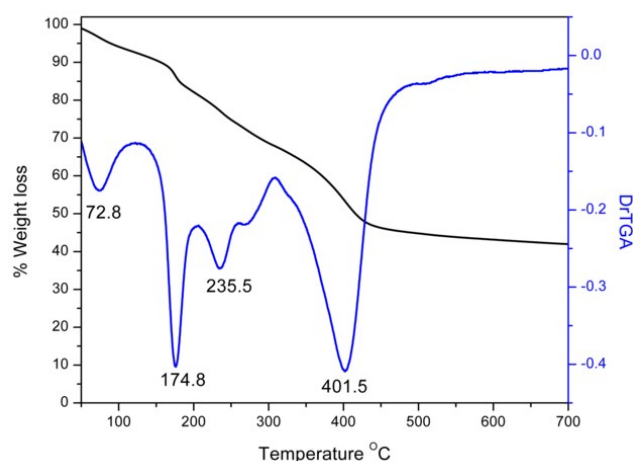


Figure 15. TG-DTG plot of PEN-G2-Cu

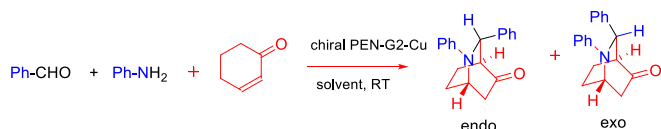
Apart from this, in the case of PEN-G2-Cu, a decomposition step with a weight loss of 25% occurs in the temperature range

of 150–250 °C. The thermal decomposition of PEN-G2 shows a weight loss of 30 % which occurs in the temperature range of 120–320 °C. From the reports regarding polyepichlorohydrin and Merrifield resin,<sup>59</sup> this decomposition is ascribed to the release of amines as nitrogen, carbonyls as CO or CO<sub>2</sub> and the degradation of the polymeric backbone to be left with a residue containing copper oxide or hydroxide. The first step of decomposition in chiral PEN-G2-Cu is attributable to the loss of non-coordinated water, occurring in the temperature range of 65–105 °C. The TG-DTG analysis data for the dendrigraft polymers are thus in agreement with the percentage composition.

## 2.4 Catalytic activity of supported chiral dendrigraft PEN-Gn-Cu complex

### 2.4.1 Synthesis of Isoquinuclidines

In a survey of catalytic activity, chiral dendrigraft PEN-G1 and G2 copper complexes were employed in the synthesis of Isoquinuclidines (Scheme 6).



**Scheme 6** Aza Diels-Alder reaction of cyclohexenone with aldimines

It was found that chiral PEN-G2-Cu catalyst was more efficient than chiral PEN-G1-Cu catalyst. A variety of aldehydes as substrates has been tried. The effects of various reaction parameters, such as type of solvent, reaction temperature, catalyst concentration, etc., were evaluated using benzaldehyde, aniline and cyclohexenone as model substrates and chiral PEN-G2-Cu as the catalyst. Optimization studies of solvent and catalyst concentration are shown in Table 3 and 4.

The reaction of cyclohexenone with imine was carried out in several solvents at an ambient temperature of 30 °C for 5h. The results are summarized in Table 3. As shown in the table, selected solvents provide the product in reasonable yield with enantiomeric excess greater than 70 %. CCl<sub>4</sub> was chosen as the preferred solvent for further studies, because the best endo/exo ratio of the product was observed in this solvent. The efficiency of the catalyst was tested by varying the catalyst concentration.

**Table 3** Optimization of solvent<sup>a</sup>

View Article Online

DOI: 10.1039/C6RA15548K

Entry	Solvent	Yield (%) <sup>b</sup>	(endo/exo) <sup>c</sup>	ee (%) <sup>d</sup>
1	DMSO	60	82/18	80
2	CCl <sub>4</sub>	82	92/08	90
3	Ethanol	78	76/24	74
4	Hexane	72	50/50	64
5	Toluene	82	60/40	75
6	THF	78	55/45	78
7	CH <sub>3</sub> CN	82	75/25	74

<sup>a</sup>Reaction Conditions: Cyclohexenone (1 mmol), benzaldehyde (1 mmol), aniline (1 mmol). RT, PEN-G2-Cu: 20 mg, <sup>b</sup>Isolated yield of endo and exo, <sup>c</sup>Determined by <sup>1</sup>H NMR, <sup>d</sup>Enantiomeric excess of the major product was determined by chiral HPLC analysis (Chiralpak IB-3 chiral stationary phase, iPrOH/hexane (1:9), 254 nm).

As shown in Table 4, there was no appreciable change in the enantiomeric excess of the major product while decreasing the catalyst loading from .01 to .005 mol %. However, the best yield and % ee were achieved at .0051 mol % of the catalyst. We have also checked the influence of the amount of solvent of the reaction mixture on the catalyst efficiency. A dilution led to a decrease of the yield but the best % ee of the product was achieved with 3 mL of carbon tetrachloride.

**Table 4** Optimization of Amount of Catalyst<sup>a</sup>

Catalyst Amount (mg)	Catalyst Amount (mol %)	Yield (%) <sup>b</sup>	TON, TOF (h <sup>-1</sup> )	(endo/exo) <sup>c</sup>	ee (%) <sup>d</sup>
2.0	.0010	53	53, 10.6	60/40	72
7.0	.0036	65	18, 3.6	75/25	74
10.0	.0051	82	16, 3.2	92/08	90
15.0	.0076	82	11, 2.2	88/12	78
20.0	.0102	82	8, 1.6	90/10	90

<sup>a</sup> Reaction Conditions: Cyclohexenone (1mmol), benzaldehyde (1mmol), aniline (1mmol). CCl<sub>4</sub>-3mL, RT, <sup>b</sup> Isolated yield of endo and exo, <sup>c</sup> Determined by <sup>1</sup>H NMR, <sup>d</sup> Enantiomeric excess of the major product was determined by chiral HPLC analysis (Chiralpak IB-3 chiral stationary phase, iPrOH/hexane (1:9), 254 nm).

Having established the optimum reaction conditions, effect of generation of the dendrigraft PEN-G<sub>n</sub>-Cu was studied (Table 5). A positive dendritic effect was observed as the % ee increased with generation of the polymer. Indeed, first generation resulted in endo/exo ratio of 75/25, the second generation furnished endo/exo product ratio with 92/08 with 90% ee.

**Table 5.** Effect of Generation of the Dendrigraft PEN-G2-Cu<sup>a</sup>

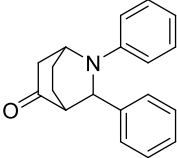
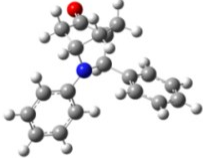
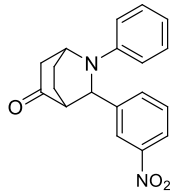
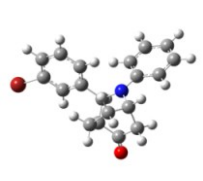
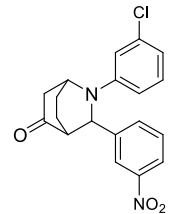
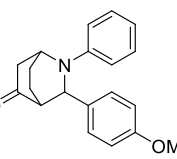
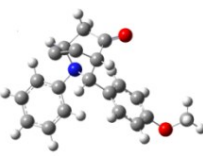
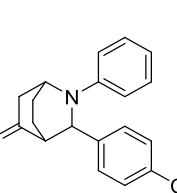
Polymer	Yield (%) <sup>b</sup>	TON, TOF (h <sup>-1</sup> )	(endo/exo) <sup>c</sup>	ee (%) <sup>d</sup>
PEN-G1-Cu	80	25, 5.0	75/25	85
PEN-G2-Cu	82	16, 3.2	92/08	90

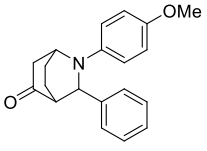
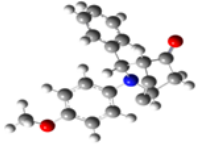
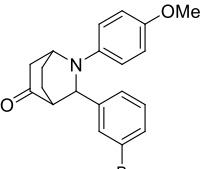
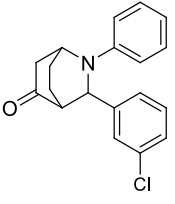
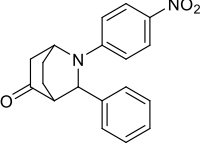
<sup>a</sup> Reaction Conditions: Cyclohexenone (1mmol), benzaldehyde (1mmol), aniline (1mmol). CCl<sub>4</sub>-3mL, RT, Catalyst amount: 10mg <sup>b</sup> Isolated yield of endo and exo, <sup>c</sup> Determined by <sup>1</sup>H NMR, <sup>d</sup> Enantiomeric excess of the major product was determined by chiral HPLC analysis (Chiralpak IB-3 chiral stationary phase, iPrOH/hexane (1:9), 254 nm).

After optimizing the reaction conditions, scope of different substrates was evaluated (Table 6). All the substrates selected were studied for 3 h. Most of the reactions of cyclohexenone with imines resulted in good diastereo and enantioselectivity irrespective of the functional group on the aromatic ring. <sup>1</sup>H NMR and GC-MS spectra of few diastereomers are shown in supplementary information. The distereomeric ratio can be found out from proton NMR spectrum as well as from the GC-MS. In GC-MS, splitting pattern corresponding to endo and exo will be different which helps to predict diastereomeric ratio.

Table 6 Scope of substrates

View Article Online  
DOI: 10.1039/C6RA15548K

Aza Diels-Alder product	Optimized structure	Yield (%) <sup>b</sup>	endo/exo <sup>c</sup>	ee (%) <sup>d</sup>
 <p>6a</p>	 <p>-864.53</p>	82	92/08	90
 <p>6b</p>	 <p>-1068.95</p>	82	88/12	84
 <p>6c</p>	 <p>-3435.51</p>	84	87/13	86
 <p>6d</p>	 <p>-1528.53</p>	62	84/16	78
 <p>6e</p>	 <p>-979.69</p>	82	88/12	88
 <p>6f</p>	 <p>-1324.78</p>	84	80/20	88

 <p>6g</p>	 <p>-979.69</p>	85	88/12	90
 <p>6h</p>	 <p>-3550.67</p>	76	90/10	86
 <p>6i</p>	 <p>-1324.79</p>	89	90/10	90
 <p>6j</p>	 <p>-1069.64</p>	68	60/40	88

View Article Online  
DOI: 10.1039/C6RA15548K

In order to find whether the yield of the Aza Diels Alder product depends on its ground state energy, structure of the products were optimized using B3LYP exchange correlation functional and 6-31G basis set.<sup>60</sup> The optimized energy ie. lowest energy of the compound to be in the stable state, is depicted in the table (Table 6). As per the energy values, the compound 6a has maximum energy; so we expect it to have low yield (endo product) compared with others. But experimental results show endo/exo ratio of 92:08. In some other cases, the experimental values are agreeable with the theoretical value. For example, compound 6h have least energy value (-3550.67) which shows yield of about 90:10. These results show that formation of Aza Diels-Alder product cannot be predicted by ground state energy values alone, but other factors (kinetic and thermodynamic factors) have to be considered in order to predict the formation of the product theoretically.

#### 2.4.2 Recyclability of the Catalyst

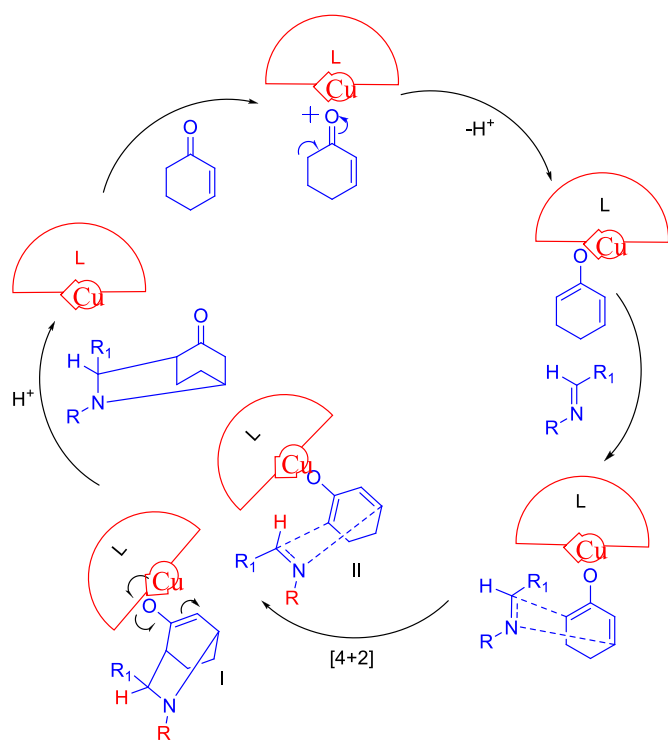
After completion of the reaction, the solution was filtered, washed with ethyl acetate (3-10 mL), acetone and vacuum dried at 50 °C for about 5h. The catalyst recovered was weighed and reused without loss of significant catalytic activity. Details regarding catalyst recovery with percentage yield are depicted in Table .7. Successive runs were carried out in order to examine the recyclability of the catalyst. After fifth cycle, 87.8 % of catalyst was recovered and reused with 74% ee.

Table 7. Recycling of chiral PEN-G2-Cu catalyst<sup>a</sup>View Article Online  
DOI: 10.1039/C6RA15548K

No. of Cycles	Catalyst weight (mg)	Catalyst recovered (mg)	Recovery (%)	Product yield (%) <sup>b</sup>	Endo/exo <sup>c</sup>	ee (%) <sup>d</sup>
1	10	9.2	92.0	82	92/08	90
2	9.2	8.4	91.3	78	82/18	82
3	8.4	7.8	92.9	74	78/22	78
4	7.8	7.4	94.9	65	75/25	74
5	7.4	6.5	87.8	65	74/26	74

### 2.4.3 The Proposed Mechanism

It is well known that a carbonyl compound possessing  $\alpha$ -hydrogens will enolize under acidic conditions and the formed enolate will attack imines formed from aldehydes and amines.



Scheme 7 Possible mechanism for Aza Diels Alder reaction of cyclohexenone with aldimines

The (4+2) diene-dienophile cycloaddition of enolate with aldimine generates intermediate I and II. Finally catalyst leaves the system to form the product, endo and exo (Scheme 7).

## 3. Experimental

### 3.1 Photolytic cleavage

Resin (500 mg) was suspended in methanol (50 mL) in the reaction chamber of an immersion type photo reactor. The suspension was degassed for 1h with dry nitrogen and irradiated with Philips HP 125W medium pressure Hg lamp at 340-350 nm for 24 h with constant stirring. A solution of CuSO<sub>4</sub> was circulated through the outer jacket of the reactor to filter off light waves below 320 nm. After photolysis, resin beads were filtered and washed with methanol. Combined filtrate and washings were evaporated under vacuum.

**G0 After photolytic cleavage:** <sup>1</sup>H NMR (400 MHz, DMSO-d<sub>6</sub>)  $\delta$ : 3.9(26 NH proton), 3.2-3.8(48 CH<sub>2</sub> & 10 CH) ppm. <sup>13</sup>C NMR (100 MHz, DMSO-d<sub>6</sub>): 78, 77.7, 70.2, 68.8, 68.6, 53.4, 51.6, 51 ppm; MALDI MS: 884.

**G1 After photolytic cleavage:** <sup>1</sup>H NMR (400 MHz, DMSO-d<sub>6</sub>)  $\delta$ : 8.2 (18 amide proton), 3.5-4 (44 NH proton), 3.1-3.4(192 CH<sub>2</sub> & 10 CH) ppm; <sup>13</sup>C NMR (100 MHz, DMSO-d<sub>6</sub>): 164.6, 56.3, 48.5, 41.2, 39.7, 39.1, 38.9, 38.6, 38.3, 37.2, 36.9, 14.1 ppm; MALDI MS: 2857.55.

**G2 After photolytic cleavage:** <sup>1</sup>H NMR (400 MHz, DMSO-d<sub>6</sub>): 8.1 (26 amide proton), 3.5-4.5 (50 NH proton), 2.8-3.5 (258 CH<sub>2</sub> & 10 CH) ppm; <sup>13</sup>C NMR (100 MHz, DMSO-d<sub>6</sub>): 168.8, 167.7, 164.6, 55, 43.4, 41.1, 40.6, 39, 38.6, 38.3, 37.2, 35.5, 28.3, 21.8, 17.5 ppm; MALDI MS: 3966.02.

### 3.2 Modification of Dendrigraft PEN-G2 Polymer with Boc Proline

Active ester of amino acid was prepared by adding 2.5 meq of HOBt (1.69 g) and 2.5 meq of DCC (2.58 g) to a solution of Boc-L-Proline (2.69 g) in NMP. This was stirred for 5 min. and the HOBt ester of amino acid was added to the amino resin, PEN-G2 (0.5 g). The mixture was shaken for 48 h until the disappearance of blue colour with ninhydrin. DMSO was added to the mixture and shaken for 15min. At the end of 15 min. DIEA was added. The unreacted reagents and byproducts were filtered off. The resin was washed with dichloromethane: methanol (66:33 v/v), dichloromethane, NMP and dried under vacuum at 50 °C.

Amount of Boc-proline: 0.021 mol g<sup>-1</sup>; Yield: 0.58 g.

IR (cm<sup>-1</sup>): 3460, 2934, 1740, 1652, 1539, 1366, 1103, 725.

Solid state  $^{13}\text{C}$  NMR (100 MHz): 172, 168.2, 167.8, 167.2, 152, 144.3, 122.2, 79.5, 76, 73, 61, 60.3, 47, 43, 38.8, 34, 29, 27, 23, 20.9 ppm.

### 3.3 Deprotection of Boc from Dendrigrraft PEN-G2 Polymer

The resin (0.5 g) was treated with 30 % TFA in dichloromethane for 5h. The reaction was monitored using ninhydrin test and IR spectrum. The TFA solution was filtered and the resin was washed with dichloromethane. This was treated with 5 % DIEA in dichloromethane (5min) & 5 % DIEA in NMP: dichloromethane mixture (1:1 v/v) to get the desired product. Finally, proline modified PEN-G2 polymer was dried at 50 °C.

Proline NH capacity: 0.021 mol/g; Yield: 0.46 g;

IR ( $\text{cm}^{-1}$ ): 3460, 2982, 1692, 1525, 1454, 1250, 1117, 750.

Solid state  $^{13}\text{C}$  NMR (100 MHz): 168, 167.5, 167, 142.3, 122.4, 79.9, 73, 64, 62.3, 49, 42, 37, 35, 30, 25, 20.2 ppm.

### 3.4 Synthesis of Copper Complex of Proline Modified Dendrigrraft PEN-G2 Polymer

A 50 mL round bottom flask was charged with 250 mg of Merrifield resin supported proline modified PEN-G2 polymer having 20.63 mmols/g of amine capacity. It was allowed to swell in DMF for 2 h. Quantitative amount of anhydrous copper acetate (0.021 mol, 0.94 g) in 10 mL methanol was added to the reaction flask. The reaction mixture was stirred at 50 °C for about two days (48h). The polymer was filtered and washed with water. The filtrate and washings were collected together and concentrated. This concentrated solution was used for the estimation of metal ions by standard methods. The polymer-supported metal complex was washed with methanol (20 mL x 3), dioxane (20 mL x 3) and acetone (20 mL x 3) followed by drying at 50 °C for 3 h.

Dark green powder; Copper loading: 0.005 mol $^{-1}$ ; Yield: 0.32 g.

### 3.5 General Procedure for Aza Diels Alder Reaction

A 25 mL RB flask was charged with a magnetic stirrer and  $\text{CCl}_4$  (3.0 mL). Cyclohexenone (1.0 mmol), and the catalyst PEN-G2-Cu (.0051 mol%, 10 mg) were added to the flask. To the resulting solution after 2 min of stirring, the Schiff base of aniline and benzaldehyde (1mmol) was added. The reaction mixture was stirred at room temperature for 3h. After the completion of the reaction (TLC and GC determination), the resulting solution was filtered, washed with ethyl acetate, methanol and acetone, and concentrated by a rotary vacuum evaporator. The product was separated by passing through a silica column using the eluent, hexane : ethyl acetate (9:1). The yield and diastereomer ratio were determined from  $^1\text{H}$  NMR spectrum. Product purification and diastereomer separation were made by column chromatography on  $\text{SiO}_2$  column (hexane/EtOAc/ $\text{Et}_3\text{N}$  40:10:1). The enantiomeric purity was determined by chiral HPLC analysis (Chiralpak IB-3 chiral stationary phase, iPrOH/hexane (1:9), 254 nm).

## 4. Conclusions

Polyepichlorohydrin was coupled to Merrifield resin in order to increase the loading capacity. Novel families of

dendrigrraft G0, G1 and G2 amine polymer, having pentaerythritol initiated polyepichlorohydrin as core have been synthesized and characterized. Characterization of dendrigrraft amidoamine polymer has been done after photolytic cleavage of the same from the support. We have developed a highly efficient chiral dendritic copper catalyzed method for the cycloaddition of cyclohexenone with aldimines. The developed copper complexes of chiral PEN-G1 and PEN-G2 dendrigrraft polymer were characterized. We found that copper complexes can catalyze Aza Diels-Alder reaction like Diels-Alder reaction. The reaction occurs more efficiently with high generation dendrigrraft polymer in comparison with low generation G1 dendrigrraft polymer. After optimizing the reaction conditions, a detailed study of aza Diels-Alder reaction was done with chiral PEN-G2 copper catalyst. The main features of the synthesis are: only small amount of catalyst was needed to drive the reaction and all the reactions were performed at room temperature. The catalyst performs well with good diastereoselectivity and good enantiomeric excess. Procedural simplicity, simple recovery and reusability of catalysts meet the requirements of benign chemistry. Thus the present catalyst will be of wide practical application in similar reactions. Further investigation on the application of this catalyst for other organic reactions is in progress.

## Acknowledgements

We would like to thank SAIF, CUSAT for assistance with various analysis. One of the authors (G.S) thank the CSIR, Govt. of India for financial assistance in the form of fellowship. The authors thank PSRT, CUSAT for GPC analysis, NCL, Pune for Solid state  $^{13}\text{C}$  NMR analysis, RGCB and NIIST, Trivandrum for MALDI analysis. Finally we thank Thermax, India for providing the gift sample of Merrifield resin.

## References

- (a) A. D. Schluter and J. P. Rabe, *Angew Chem. Int. Ed.* 2000, **39**, 864-883; (b) A. D. Schluter, *J. Polym. Sci., Part A: Polym Chem.*, 2001, **39**, 1533-1556; (c) A. F. Zhang, L. J. Shu, Z. S. Bo and A. D. Schluter, *Macromol Chem. Phys.*, 2003, **204**, 328-339; (d) H. Frauenrath, *Prog. Polym. Sci.*, 2005, **30**, 325-384; (e) C. C. Lee, J. A. MacKay, J. M. J. Frechet and F. C. Szoka, *Nat. Biotechnol.*, 2005, **23**, 1517-1526; (f) J. G. Rudick and V. Percec, *Acc. Chem. Res.*, 2008, **41**, 1641-1652; (g) B. M. Rosen, C. J. Wilson, D. A. Wilson, M. Peterca, M. R. Imam and V. Percec, *Chem. Rev.*, 2009, **109**, 6275-6540; (h) W. Li, A. Zhang and A. D. Schlueter, *Macromolecules*, 2008, **41**, 43-49; (i) W. Li, A. Zhang, K. Feldman, P. Walde and A. D. Schlueter, *Macromolecules*, 2008, **41**, 3659-3667; (j) W. Zhuang, E. Kasemi, Y. Ding, M. Kroeger, A. D. Schlueter and J. P. Rabe, *Adv. Mater.*, 2008, **20**, 3204-+; (k) A. J. Boydston, T. W. Holcombe, D. A. Unruh, J. M. J. Frechet and R. H. Grubbs, *J. Am. Chem. Soc.*, 2009, **131**, 5388-+; (l) Y. Guo, J. D. van Beek, B. Zhang, M. Colussi, P. Walde, A. Zhang, M. Kroeger, A. Halperin and A. D.

- Schlueter, *J. Am. Chem. Soc.*, 2009, **131**, 11841-11854; (m) I. Popa, B. Zhang, P. Maroni, A. D. Schlueter and M. Borkovec, *Angew. Chem. Int. Ed.*, 2010, **49**, 4250-4253; (n) B. Zhang, R. Wepf, K. Fischer, M. Schmidt, S. Besse, P. Lindner, B. T. King, R. Sigel, P. Schurtenberger, Y. Talmon, Y. Ding, M. Kroeger, A. Halperin and A. D. Schlueter, *Angew. Chem. Int. Ed.*, 2011, **50**, 737-740; (o) R. M. England and S. Rimmer, *Polym. Chem.*, 2010, **1**, 1533-1544; (p) Y. Deng, S. Zhang, G. Lu and X. Huang, *Polym. Chem.*, 2013, **4**, 1289-1299; (q) C. Li, H. Liu, D. Tang and Y. Zhao, *Polym. Chem.*, 2015, **6**, 1474-1486; (r) C. Guo, L. Sun, W. She, N. Li, L. Jiang, K. Luo, Q. Gong and Z. Gu, *Polym. Chem.*, 2016, **7**, 2531-2541.
- J. S. Fruchtel and G. Jung, *Angew. Chem. Int. Ed.*, 1996, **35**, 17-42.
  - G. Smitha and K. Sreekumar, *RSC Adv.*, 2016, **6**, 18141-18155.
  - (a) R. Haag, *Chem. Eur. J.*, 2001, **7**, 327-335; (b) S. Lebreton, S. Monaghan and M. Bradley, *Aldrichim. Acta*, 2001, **34**, 75-83.
  - V. Swali, N. J. Wells, G. J. Langley and M. Bradley, *J. Org. Chem.*, 1997, **62**, 4902-4903.
  - D. A. Tomalia, H. Baker, J. Dewald, M. Hall, G. Kallos, S. Martin, J. Roeck, J. Ryder and P. Smith, *Polym. J.*, 1985, **17**, 117.
  - N. J. Wells, A. Basso and M. Bradley, *Biopolymers*, 1998, **47**, 381-396.
  - N. J. Wells, M. Davies and M. Bradley, *J. Org. Chem.*, 1998, **63**, 6430-6431.
  - (a) A. Dahan and M. Portnoy, *J. Am. Chem. Soc.*, 2007, **129**, 5860-5869; (b) T. Kehat, K. Goren and M. Portnoy, *New J. Chem.*, 2007, **31**, 1218-1242; (c) A. Y.-T. Huang, C.-H. Tsai, H.-Y. Chen, H.-T. Chen, C.-Y. Lu, Y.-T. Lin and C.-L. Kao, *Chem. Commun.*, 2013, **49**, 5784-5786; (d) R. K. G. Panicker and S. Krishnapillai, *Tetrahedron Lett.*, 2014, **55**, 2352-2354; (e) P. Arya, N. V. Rao, J. Singkhonrat, H. Alper, S. C. Bourque and L. E. Manzer, *J. Org. Chem.*, 2000, **65**, 1881-1885; (f) S. Lebreton, N. Newcombe and M. Bradley, *Tetrahedron Lett.*, 2002, **43**, 2475-2478; (g) J. Lu and P. H. Toy, *Chem. Rev.*, 2009, **109**, 815-838; (h) E. Delort, N.-Q. Nguyen-Trung, T. Darbre and J.-L. Reymond, *J. Org. Chem.*, 2006, **71**, 4468-4480; (i) J. J. Diaz-Mochon, M. A. Fara, R. M. Sanchez-Martin and M. Bradley, *Tetrahedron Lett.*, 2008, **49**, 923-926; (j) K. Goren and M. Portnoy, *Chem. Commun.*, 2010, **46**, 1965-1967; (k) T. Kehat and M. Portnoy, *Chem. Commun.*, 2007, 2823-2825; (l) L. Tuchman-Shukron and M. Portnoy, *Adv. Synth. Catal.*, 2009, **351**, 541-546; (m) M. P. Kapoor, Y. Kasama, T. Yokoyama, M. Yanagi, S. Inagaki, N. Hironobu and L. R. Juneja, *J. Mater. Chem.*, 2006, **16**, 4714-4722; (n) G. R. Krishnan and K. Sreekumar, *Eur. J. Org. Chem.*, 2008, 4763-4768; (o) J.-P. Lindner, C. Roeben, A. Studer, M. Stasiak, R. Ronge, A. Greiner and H.-J. Wendorff, *Angew. Chem. Int. Ed.*, 2009, **48**, 8874-8877; (p) G. R. Krishnan and K. Sreekumar, *Polymer*, 2008, **49**, 5233-5240; (q) A.-M. Caminade, A. Ouali, M. Keller and J.-P. Majoral, *Chem. Soc. Rev.*, 2012, **41**, 4113-4125.
  - (a) G. Consiglio, *In Catalytic Asymmetric Synthesis, I. Ojima Ed., VCH, New York*, 1993; (b) R. Noyori, *Asymmetric Catalysis in Organic Synthesis, John Wiley & Sons, New York*, 1994; (c) M. Rueping, B. J. Nachtsheim, W. leawsuwan and I. Atodiresei, *Angew. Chem. Int. Ed.*, 2011, **50**, 6706-6720; (d) V. Eschenbrenner, L. S. Kumar and H. Waldmann, *Angew. Chem. Int. Ed.*, 2014, **53**, 11146-11157; (e) Z. Y. Cao, W. D. G. Brittain, J. S. Fossey and F. Zhou, *Catal. Sci. Tech.*, 2015, **5**, 3441-3451.
  - (a) M. G. Memeo and P. Quadrelli, *Chem. Eur. J.*, 2012, **18**, 12554-12582; (b) S. Kobayashi and H. Ishitani, *Chem. Rev.*, 1999, **99**, 1069-1094; (c) H. B. Kagan and O. Riant, *Chem. Rev.*, 1992, **92**, 1007-1019; (d) K. A. Jorgensen, *Angew. Chem. Int. Ed.*, 2000, **39**, 3558-3588.
  - (a) A. D. Schluter, in *Functional Molecular Nanostructures, Top. Curr. Chem.*, 2005, **245**, 151-191; (b) K. Ishitani, K. Tsubaki, A. Mori and S. Uchida, *Prog. Polym. Sci.*, 2003, **28**, 27-54.
  - (a) T. Akiyama, J. Itoh and K. Fuchibe, *Adv. Synth. Catal.*, 2006, **348**, 999-1010; (b) J. Itoh, K. Fuchibe and T. Akiyama, *Angew. Chem. Int. Ed.*, 2006, **45**, 4796-4798; (c) U. K. Tambar, S. K. Lee and J. L. Leighton, *J. Am. Chem. Soc.*, 2010, **132**, 10248-10250; (d) S. Kobayashi, S. Komiyama and H. Ishitani, *Angew. Chem. Int. Ed.*, 1998, **37**, 979-981; (e) S. Kobayashi, K. Kusakabe and H. Ishitani, *Org. Lett.*, 2000, **2**, 1225-1227; (f) S. Kobayashi, K. Kusakabe, S. Komiyama and H. Ishitani, *J. Org. Chem.*, 1999, **64**, 4220-4221; (g) Y. Yamashita, Y. Mizuki and S. Kobayashi, *Tetrahedron Lett.*, 2005, **46**, 1803-1806; (h) N. S. Josephsohn, M. L. Snapper and A. H. Hoveyda, *J. Am. Chem. Soc.*, 2003, **125**, 4018-4019; (i) O. G. Mancheno, R. G. Arrayas and J. C. Carretero, *J. Am. Chem. Soc.*, 2004, **126**, 456-457; (j) S. L. Yao, S. Saaby, R. G. Hazell and K. A. Jorgensen, *Chem. Eur. J.*, 2000, **6**, 2435-2448; (k) M. S. Taylor and E. N. Jacobsen, *Angew. Chem. Int. Ed.*, 2006, **45**, 1520-1543; (l) Y. Takemoto, *Org. Biomol. Chem.*, 2005, **3**, 4299-4306; (m) A. K. Unni, N. Takenaka, H. Yamamoto and V. H. Rawal, *J. Am. Chem. Soc.*, 2005, **127**, 1336-1337.
  - (a) D. Uraguchi and M. Terada, *J. Am. Chem. Soc.*, 2004, **126**, 5356-5357; (b) T. Akiyama, H. Morita, J. Itoh and K. Fuchibe, *Org. Lett.*, 2005, **7**, 2583-2585; (c) R. I. Storer, D. E. Carrera, Y. Ni and D. W. C. MacMillan, *J. Am. Chem. Soc.*, 2006, **128**, 84-86; (d) J. Seayad, A. M. Seayad and B. List, *J. Am. Chem. Soc.*, 2006, **128**, 1086-1087; (e) D. Uraguchi, K. Sorimachi and M. Terada, *J. Am. Chem. Soc.*, 2005, **127**, 9360-9361; (f) M. Terada, K. Machioka and K. Sorimachi, *Angew. Chem. Int. Ed.*, 2006, **45**, 2254-2257; (g) M. Rueping, A. R. Antonchick and T. Theissmann, *Angew. Chem. Int. Ed.*, 2006, **45**, 2617-2619; (h) S. Mayer and B. List, *Angew. Chem. Int. Ed.*, 2006, **45**, 4193-4195; (i) X.-H. Chen, X.-Y. Xu, H. Liu, L.-F. Cun and L.-Z. Gong, *J. Am. Chem. Soc.*, 2006, **128**, 14802-14803.
  - H. Ishitani and S. Kobayashi, *Tetrahedron Lett.*, 1996, **37**, 7357-7360.
  - (a) H. Ishitani, M. Ueno and S. Kobayashi, *J. Am. Chem. Soc.*, 1997, **119**, 7153-7154; (b) K. Hattori and H. Yamamoto, *Tetrahedron* 1993, **49**, 1749-1760.
  - S. K. Lee, U. K. Tambar, N. R. Perl and J. L. Leighton, *Tetrahedron*, 2010, **66**, 4769-4774.
  - W. Zhang, Y. Dai, X. Wang and W. Zhang, *Tetrahedron Lett.*, 2011, **52**, 6122-6126.
  - Z. Chen, L. Lin, D. Chen, J. Li, X. Liu and X. Feng, *Tetrahedron Lett.*, 2010, **51**, 3088-3091.

20. H. Shirakawa and H. Sano, *Tetrahedron Lett.*, 2014, **55**, 4095-4097.
21. H. Sunden, I. Ibrahim, L. Eriksson and A. Cordova, *Angew. Chem. Int. Ed.*, 2005, **44**, 4877-4880.
22. H. Liu, L.-F. Cun, A.-Q. Mi, Y.-Z. Jiang and L.-Z. Gong, *Org. Lett.*, 2006, **8**, 6023-6026.
23. V. I. Maleev, T. y. V. Skrupskaya, L. V. Yashkina, A. F. Mkrtchyan, A. S. Saghyan, M. M. Il'in and D. A. Chusov, *Tetrahedron-Asymmetry*, 2013, **24**, 178-183.
24. H. Yamamoto, *Lewis Acids in Organic Synthesis*, Wiley-VCH, 2000.
25. F. M. Menger and T. Tsuno, *J. Am. Chem. Soc.*, 1989, **111**, 4903-4907.
26. (a) C. C. Mak and H. F. Chow, *Macromolecules*, 1997, **30**, 1228-1230; (b) H. F. Chow and C. C. Mak, *J. Org. Chem.*, 1997, **62**, 5116-5127.
27. K. I. Fujita, T. Muraki, H. Hattori and T. Sakakura, *Tetrahedron Lett.*, 2006, **47**, 4831-4834.
28. (a) L. He, G. Laurent, P. Retailleau, B. Folleas, J.-L. Brayer and G. Masson, *Angew. Chem. Int. Ed.*, 2013, **52**, 11088-11091; (b) S. Reymond and J. Cossy, *Chem. Rev.*, 2008, **108**, 5359-5406.
29. (a) K. Juhl and K. A. Jorgensen, *Angew. Chem. Int. Ed.*, 2003, **42**, 1498-1501; (b) Y. Yamamoto, N. Momiyama and H. Yamamoto, *J. Am. Chem. Soc.*, 2004, **126**, 5962-5963; (c) Y. Hayashi, J. Yamaguchi, K. Hibino, T. Sumiya, T. Urushima, M. Shoji, D. Hashizume and H. Koshino, *Adv. Synth. Catal.*, 2004, **346**, 1435-1439; (d) A. B. Northrup and D. W. C. MacMillan, *J. Am. Chem. Soc.*, 2002, **124**, 2458-2460; (e) D. B. Ramachary, N. S. Chowdari and C. F. Barbas, *Angew. Chem. Int. Ed.*, 2003, **42**, 4233-4237; (f) K. A. Ahrendt, C. J. Borths and D. W. C. MacMillan, *J. Am. Chem. Soc.*, 2000, **122**, 4243-4244; (g) H. Sunden, N. Dahlin, I. Ibrahim, H. Adolfsson and A. Cordova, *Tetrahedron Lett.*, 2005, **46**, 3385-3389.
30. (a) J. Casas, M. Engqvist, I. Ibrahim, B. Kaynak and A. Cordova, *Angew. Chem. Int. Ed.*, 2005, **44**, 1343-1345; (b) A. Cordova, H. Sunden, M. Engqvist, I. Ibrahim and J. Casas, *J. Am. Chem. Soc.*, 2004, **126**, 8914-8915; (c) H. Sunden, M. Engqvist, J. Casas, I. Ibrahim and A. Cordova, *Angew. Chem. Int. Ed.*, 2004, **43**, 6532-6535; (d) A. Cordova, *Acc. Chem. Res.*, 2004, **37**, 102-112; (e) A. Bøgevig, H. Sunden and A. Cordova, *Angew. Chem. Int. Ed.*, 2004, **43**, 1109-1112; (f) A. Cordova, *Chem. Eur. J.*, 2004, **10**, 1987-1997; (g) A. Cordova, H. Sunden, A. Bøgevig, M. Johansson and F. Himo, *Chem. Eur. J.*, 2004, **10**, 3673-3684.
31. K. U. Ito, *Polym. J.*, 1979, **11**, 171-174.
32. R. B. Merrifield, *J. Am. Chem. Soc.*, 1963, **85**, 2149-2151.
33. (a) A. Barbara, *Tetrahedron Lett.*, 1973, **14**, 21-25; (b) J. Karabline and M. Portnoy, *Org. Biomol. Chem.*, 2012, **10**, 4788-4794.
34. S. K. Sahu, S. P. Panda, D. S. Sadafule, C. G. Kumbhar, S. G. Kulkarni and J. V. Thakur, *Polym. Degrad. Stab.*, 1998, **62**, 495-500.
35. B. Gaur, B. Lochab, V. Choudhary and I. K. Varma, *J. Macromol. Sci. Polymer Rev.*, 2003, **C43**, 505-545.
36. H. J. Milton, E. C. Struck, M. G. Case and P. M. Steven, *J. Polym. Sci. A Polym. Chem.*, 1984, **22**, 341-352.
37. (a) T. Biedron, P. Kubisa and S. Penczek, *J. Polym. Sci., Part A: Polym. Chem.*, 1991, **29**, 619-628; (b) G. Ampleman, *US Patent*, 1992, 5,124,463.
38. P. Liu, *Anal. Chim. Acta*, 2005, **95**, 695-698.
39. H. Arisawa and T. B. Brill, *Combust. Flame*, 1998, **112**, 533-544.
40. D. A. Tomaia, *Macromolecules*, 1986, **19**, 2466-2472.
41. F. Guillier, D. Orain and M. Bradley, *Chem. Rev.*, 2000, **100**, 2091-2157.
42. F. P. Luiz, R. Ricardo and F. M. Eduardo, *J. Am. Chem. Soc.*, 2013, **135**, 11513-11516.
43. L. Shu, *Dendronized Polystyrene: Synthesis, Characterization and SFM Investigations of Cylindrical Nanoobjects*, 2001, Ph.D. Dissertation, University of Berlin, Germany.
44. (a) D. C. Schriemer and L. Li, *Anal. Chem.*, 1997, **69**, 4176-4183; (b) A. M. Schaiberger and J. A. Moss, *J. Am. Soc. Mass Spe.*, 2008, **19**, 614-619; (c) U. Bahr, A. Deppe, M. Karas, F. Hillenkamp and U. Giessmann, *Anal. Chem.*, 1992, **64**, 2866-2869.
45. D. A. Tomalia and J. M. J. Frechet, *Dendrimers and Dendritic Polymers*, 2001, Wiley series in Polymer Science, 587-604.
46. S. S. Sheiko and M. Moller, *Chem. Rev.*, 2001, **101**, 4099-4123.
47. N. Thi-Thanh-Tam, B. Martin, R. Ali, J. R. Hans, I. Lieberwirth and K. Mullen, *J. Am. Chem. Soc.*, 2013, **135**, 4183-4186.
48. M. F. Ottaviani, S. Bossmann, N. J. Turro and D. A. Tomalia, *J. Am. Chem. Soc.*, 1994, **116**, 661-671.
49. E.-H. Kang, I. S. Lee and T.-L. Choi, *J. Am. Chem. Soc.*, 2011, **133**, 11904-11907.
50. A. M. Naylor, W. A. Goddard, G. E. Kiefer and D. A. Tomaia, *J. Am. Chem. Soc.*, 1989, **111**, 2339-2341.
51. A. Carlmark, E. Malmstrom and M. Malkoch, *Chem. Soc. Rev.*, 2013, **42**, 5858-5879.
52. J. Li, L. T. Piehler, D. Qin, J. R. Baker, Jr. and D. A. Tomalia, *Langmuir*, 2000, **16**, 5613-5616.
53. L. J. Shu, T. Schafer and A. D. Schluter, *Macromolecules*, 2000, **33**, 4321-4328.
54. D. Xie, M. Jiang, G. Zhang and D. Chen, *Chem. Eur. J.*, 2007, **13**, 3346-3353.
55. L. Zhou, D. H. Russell, M. Q. Zhao and R. M. Crooks, *Macromolecules*, 2001, **34**, 3567-3573.
56. (a) S. Thakurta, P. Roy, G. Rosair, C. J. Gomez-Garcia, E. Garribba and S. Mitra, *Polyhedron*, 2009, **28**, 695-702; (b) V. P. Singh, *Spectrochim Acta Part A*, 2008, **71**, 17-19.
57. M. C. Biesinger, L. W. M. Lau, A. R. Gerson and R. S. C. Smart, *Appl. Surf. Sci.*, 2010, **257**, 887-898.
58. S. K. Sahu, S. P. Panda, D. S. Sadafule, C. G. Kumbhar, S. G. Kulkarni and J. V. Thakur, *Polym. Degrad. Stab.*, 1998, **62**, 495-500.
59. S. Pisharath and H. G. Ang, *Polym. Degrad. Stab.*, 2007, **92**, 1365-1377.
60. (a) A. D. Becke, *J. Chem. Phys.*, 1993, **98**, 5648-5652; (b) P. J. Stephens, F. J. Devlin, C. F. Chabalowski and M. J. Frisch, *J. Phys. Chem.*, 1994, **98**, 11623-11627.

## Chiral dendrigraft polymer for asymmetric synthesis of isoquinuclidines

G. Smitha, K. Sreekumar\*

Synthesis of copper complex of chiral modified dendrigraft amidoamine polymer with pentaerythritol initiated polyepichlorohydrin core, PEN-G2 has been demonstrated on a solid resin support for the synthesis of isoquinuclidines via Aza Diels-Alder reaction between cyclohexenone and imines.

